Particle dynamics and the development of string-like motion in a simulated monoatomic supercooled liquid

Y. Gebremichael[a)]
Departments of Chemical Engineering and Materials Science and Engineering, University of Michigan, Ann Arbor, Michigan 48109

M. Vogel and S. C. Glotzer[b)]
Departments of Chemical Engineering and Materials Science and Engineering, University of Michigan, Ann Arbor, Michigan 48109

The microscopic details of local particle dynamics is studied in a glass-forming one component supercooled liquid modeled by a Dzugutov potential developed for simple metallic glass formers. Our main goal is to investigate particle motion in the supercooled liquid state, and to ascertain the extent to which this motion is cooperative and occurring in quasi-one-dimesional, string-like paths. To this end we investigate in detail the mechanism by which particles move along these paths. In particular, we show that the degree of coherence—that is, simultaneous motion by consecutive particles along a string—depends on the length of the string. For short strings, the motion is highly coherent. For longer strings, the motion is highly coherent only within shorter segments of the string, which we call "microstrings." Very large strings may contain several microstrings within which particles move simultaneously, but individual microstrings within a given string are temporally uncorrelated with each other. We discuss possible underlying mechanism for this complex dynamical behavior, and examine our results in the context of recent work by Garrahan and Chandler [Phys. Rev. Lett. **89**, 035704 (2002)] in which dynamic facilitation plays a central role in the glass transition.   © *2004 American Institute of Physics.* [DOI: 10.1063/1.1644539]

I. INTRODUCTION

The increasing complexity in the dynamics of liquids cooled towards their glass transition has received much attention.[1–8] It has been demonstrated in simulations[9–21] and experiments[22–30] that both stretched exponential relaxation and the decoupling of transport coefficients in supercooled liquids are to a large extent a consequence of the emergence of dynamical heterogeneity upon cooling.[31–33] Physical regions in these liquids consist of subensembles of particles that have temporarily enhanced or diminished mobility relative to the average.[34–36] Those particles that have enhanced mobility aggregate into clusters that grow in size with decreasing temperature. This has been demonstrated through a number of computational,[16,19,21] and also experimental[28] studies. A closer inspection of these clusters reveals that, within any cluster of mobile particles, smaller subsets move together in a correlated fashion where several particles replace each other along one-dimensional, "string-like" paths.[10] It has been speculated that these strings are the elementary unit of cooperative motion[36] originally envisioned by Adam and Gibbs.[37]

Previously, the existence of these dynamically correlated structures, and the transient nature and T dependence of the average string size, were studied in simulations of a Lennard-Jones (LJ) binary mixture[10] and a polymer melt.[20] The mean string size was shown to have a maximum during the period when the dynamical heterogeneity as measured in terms of the non-Gaussian parameter is most pronounced. Similarly correlated structures were also observed in the simulation of a nonrandomly frustrated model of spin glasses that are perceived as a model for glass formers.[38] Experimentally, a number of studies find direct and indirect evidence for dynamically correlated groups of particles. Using an approach that corrects multiple scattering noise in inelastic coherent neutron scattering experiments, Russina and Mezei[30,39] explored the microscopic dynamics of a supercooled liquid at small wave numbers and found evidence for collective fast atomic motion on the scale of the intermediate range order found in the static structure. In view of the spatially extended character of the collective excitations, they argued that they may be evidence for strings. A direct experimental observation of string-like motion was made by Marcus *et al.*[27] and Cui *et al.*[40] in concentrated quasi-two-dimensional colloidal liquids. Using three-dimensional (3D) confocal microscopy, Weeks and Weitz[41] showed unidirectional motion of neighboring particles in colloidal systems and attributed these motions in part to string-like particle rearrangements.

The concept of string-like motion plays an important role in the development of new emerging theories, as well as in more traditional theories of the glass transition. For example Garrahan and Chandler[42,43] and Berthier and Garrahan,[44,45] have recently provided a "nontopographic"

[a)]Permanent address: Chemical Physics Program, Institute for Physical Sciences and Technology, University of Maryland, College Park, MD 20742-2431.
[b)]Author to whom correspondence should be addressed. Electronic mail: sglotzer@umich.edu

description of dynamics in supercooled liquids. Central to the theory is the notion of dynamic facilitation, originally introduced by Fredrickson and Andersen.[46,47] Dynamic facilitation corresponds to the idea that when particles in a microscopic region of space are mobile, they influence the dynamics of particles in neighboring regions, enabling them to become mobile, thereby allowing mobility to propagate through the system.[44,45] It has been argued that the observation that highly mobile particles in a supercooled liquid move along correlated strings is a confirmation of this central idea.[44] Previous analysis of the system studied in the present paper indeed suggests that clusters of highly mobile particles are formed as a result of mobility propagation initiated within a nanoscopic local structure and facilitated through quasi-one-dimensional string-like rearrangements.[48]

String-like rearrangement of particles has also been recognized in the potential energy landscape or ''topographic'' view point of dynamics in supercooled liquids.[49–52] In this picture, the structural relaxation of particles at sufficiently low temperatures is attributed to transitions between local energy minima, or inherent structures, of the multidimensional potential energy hypersurface. In fragile liquids, similar to the scenario described in terms of multifunnel structures,[53,54] basins in configuration space are organized into ''metabasins.''[50,52] Büchner and Heuer[56] and Doliwa and Heuer[57] recently showed that, upon deep supercooling, a liquid becomes trapped in a single metabasin for an extended period of time, making frequent hops within the metabasin, and infrequent excursions from one metabasin to another. Schrøder et al.[58] showed that transitions between inherent structures involve string-like motion. Further, Denny et al.[59] observed that transitions between metabasins involve cooperative rearrangement of particles. The relevance of string-like motion during inherent structure and metabasin transitions was recently investigated in detail by Vogel et al.[60] It was demonstrated that although string-like motion facilitates both types of transitions, it is of particular importance for metabasin transitions. All these studies suggest that the concept of string-like motion is essential for understanding how particle rearrangements lead to exploration of configuration space.

Perhaps the most well-known theory that connects dynamical properties of supercooled liquids to their thermodynamic properties is the Adam–Gibbs theory.[37] The main prediction of the theory relates the structural relaxation time τ_α to the configurational entropy S_c through the relation $\tau_\alpha \sim \exp[1/(TS_c)]$. This relation has been tested in simulations and appears to be valid across a wide spectrum of liquids.[61–64] Despite the validity of the theory, the cooperatively rearranging regions (CRR) that are central to the theory and that are related to the configurational entropy, have not been definitively identified. It is reasonable to propose[36] that the CRR are associated with the mobile regions of the supercooled liquid. Indeed, a recent study[21] demonstrated a connection between the Adam–Gibbs theory and spatially heterogeneous dynamics in simulations of water. In particular, they showed that the average size of clusters of mobile particles, defined as in Ref. 16, is related to the size of the CRR.[21] Since we know that clusters are also comprised of strings,[10] a fundamental connection between strings and the CRR of Adam and Gibbs is likely, but remains to be shown.

The above examples clearly demonstrate the relevance of string-like rearrangements both in new and well-established theories of the glass transition. Nevertheless, little is known about the microscopic details of this dynamical pattern. For example, it is still elusive as to how the short time rattling motion of particles within their temporary cages evolves into structured correlated motion that is manifested as string-like motion along a one-dimensional path. In particular, it is important for the further development of these theories to understand the mechanisms involved in the formation of these local excitations, e.g., how these motions occur, how large strings develop, and to what extent the motion is coherent and cooperative. To investigate these questions, we performed a detailed microscopic analysis of string-like motion in a one-component glass-forming liquid described by the Dzugutov potential, at temperatures above the mode coupling temperature T_{MCT}. Our analysis answers several of the above questions and provides insight into the most probable mechanism for the formation of strings. The paper is organized as follows: The model used for our simulations is described in Sec. II. In Sec. III, we briefly characterize the bulk dynamics to ascertain the dynamical properties of the system at several temperatures above and below the onset of supercooling. The average properties of the mobile particles are also studied in this section to establish a basis for the detailed analysis of the mechanism for the development of string-like motion described in Sec. IV. We close by drawing our conclusions in Sec. V.

II. MODEL AND SIMULATION

A. Model

The model used in our simulations is a monoatomic system described by the Dzugutov potential,[65] which is designed to prevent the nucleation of the ground state crystal structures. This potential evolved from a pair potential that was originally developed for metallic liquids.[66] In the original potential, the parameters were optimized to reproduce the static structure factor $S(q)$ of liquid lead measured in a neutron scattering experiment close to the melting point $T_{\mathrm{m}} = 623$ K. This pair potential includes, in addition to terms describing the strong short-range interactions and the usually predicted Friedel oscillation,[67] a soft repulsive component representing the screened Coulomb repulsion between the ions.

In its present form, the Dzugutov potential is characterized by the presence of two repulsive regimes and one attractive region. Its main repulsive part is identical to that of the LJ potential, but the Dzugutov potential features an additional maximum at a range typical of next-nearest-neighbor coordination distances in closed-packed crystals.[68] This maximum suppresses crystallization by disfavoring closed-packed ordering. On the other hand, the maximum is located in a region between the distances bounded by the first and the second neighbor shells in the icosahedral polytope,[65,69] causing the preferred local order in the system to be icosa-

TABLE I. Parameters of the Dzugutov pair potential.

m	A	c	a	B	d	b
16	5.82	1.1	1.87	1.28	0.27	1.94

role in the glass formation of some simple systems,[69–71] since the "frustration" inherent in packing icosahedra in Euclidean three-dimensional space makes it impossible to form a long-range crystalline structure in which each atom has such an environment. Hence, a system described by the Dzugutov potential is a good glass former, and can be studied in the supercooled regime prior to nucleation of the crystal. Near and below T_g this system is known to exhibit a first sharp diffraction peak and a split second peak in the structure factor.[72] These are common features of metallic glasses, which have an inherent structure that can be accounted for by icosahedral coordination of the first neighbor shell. These systems are, however, multicomponent systems whose structure is mostly dictated by the presence of short-range chemical ordering. The Dzugutov liquid can thus be perceived as a one-component reference system for multicomponent metallic glass formers, whose relaxation on supercooling involves both topological and chemical ordering. Hence, the model provides a unique opportunity in separating the contribution of these processes to the formation of glasses.

The explicit form of the Dzugutov pair potential is expressed as[65]

$$V = V_1 + V_2,$$

$$V_1 = A(r^{-m} - B)\exp\left(\frac{c}{r-a}\right), \quad r < a,$$

$$V_1 = 0, \quad r \geq a, \tag{1}$$

$$V_2 = B \exp\left(\frac{d}{r-b}\right), \quad r < b,$$

$$V_2 = 0, \quad r \geq b,$$

where the parameters are compiled in Table I. In Fig. 1(a), we plot the Dzugutov potential together with the LJ potential, where the latter is shifted up by an amount 0.419ϵ to align the minima for the sake of comparison. Both potentials

have minima at the same position, but unlike the LJ potential, the Dzugutov potential has an additional repulsive piece. Figure 1(b) shows the pair correlation function $g(r)$ of a 17 576-particle Dzugutov liquid at $T = 0.42$ and $\rho = 0.85$, and shows a split second peak as observed by Dzugutov et al.[72]

The Dzugutov model has been used in studies of supercooled liquids[65,72,73] as well as in simulations of freezing,[74,75] where the observed solid structure for sufficiently long relaxation upon supercooling is found to be a monoatomic dodecagonal quasicrystal. By construction, however, such transformation can be delayed, and the potential stabilizes the one-component liquid in a metastable supercooled state, allowing a time window long enough for the observation of the essential dynamical properties. In terms of its glass transition behavior, the model is known to be a fragile liquid.[72] The supercooled regime, characterized by the super-Arrhenius slowing down of the diffusion coefficient D, is found to set in at around $T = 0.8$.[72] The critical temperature of MCT, estimated from a power law fitting of D, is $T_{MCT} = 0.4$.[72] It has been shown[72] that the onset of supercooled dynamics is accompanied by a significant change in the features of the inherent structures, where structurally distinct domains have been observed. Specifically, it has been demonstrated that the local icosahedral configurations form extended domains the size of which grows as the glass transition is approached.[76] These configurations are observed to show a tendency for low-dimensional growth, and eventually percolate below T_{MCT} leading to a dramatic increase in the structural relaxation relative to the diffusion.[72,73] It has been further shown that the structural heterogeneity is accompanied by dynamical heterogeneity, where particles initially inside the icosahedral clusters are found to have less mobility than those in the nonicosahedral environment.[73]

B. Simulation

Our molecular dynamics (MD) simulations are performed for a system of 17 576 particles in a temperature range 0.42–1.0. For all state points studied, the simulations are done under isothermal conditions and at a constant density $\rho = 0.85$ (NVT ensemble). Periodic boundary conditions are used in all three spatial directions. To prepare the system, the liquid is cooled and equilibriated in a stepwise manner
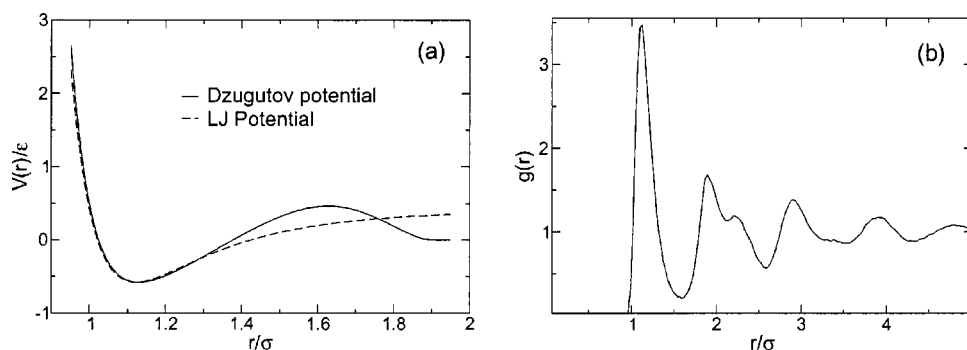

FIG. 1. (a) Dzugutov potential plotted together with LJ potential, where the LJ potential has been shifted up by 0.419ϵ to emphasize that the two potentials have minima at the same position. The Dzugutov potential has a maximum at a distance $r \approx 1.6\sigma$. (b) The pair correlation function $g(r)$ of the Dzugutov liquid at $T = 0.42$.
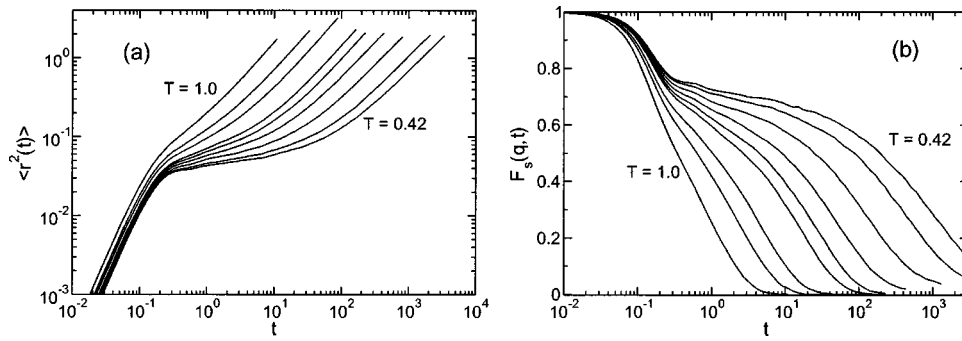
FIG. 2. (a) Mean square displacement $\langle r^2(t)\rangle$, and (b) self-intermediate scattering function $F_s(q,t)$ plotted as a function of time for different temperatures. $F_s(q,t)$ is evaluated at $q=6.82$, which corresponds to the maximum of $S(q)$. The temperatures from left to right are $T=1.0, 0.75, 0.65, 0.55, 0.52, 0.49, 0.46, 0.43,$ and 0.42.

starting from $T=1.6$. At each T studied, several independent samples are prepared to improve statistics. All analysis of bulk dynamic properties is conducted over the entire range of T, however, our detailed study of string-like motion is restricted to the lowest temperature simulated, $T=0.42$. The integration time step used in the simulation is 0.01. All units are quoted in LJ reduced units: length in units of σ, temperature T in units of ϵ/k_B, and time in units of $\sigma\sqrt{m/\epsilon}$. The mass m and the distance σ are set to unity. The simulations carried out for the present study, prior to postanalysis, required roughly 1300 cpu hours on a AMD Athlon 2000+ MP Myrinet cluster.

III. DYNAMICS OF THE BULK

In order to demonstrate that the system studied shows typical glass-forming liquid behavior we show the mean square displacement (MSD) and the incoherent (self) intermediate scattering function $F_s(q,t)$. The typical time regimes observed for these quantities will also serve us in marking and comparing the time scales relevant in the later analysis of string-like motion, which is the main goal of our study. Figure 2(a) shows the MSD for the Dzugutov liquid at different temperatures. Typical of supercooled liquids, the ballistic and diffusive regimes at short and long times, respectively, are separated by a plateau regime at intermediate times. The plateau, which results from the temporary "caging" of each particle by its neighbors, extends to longer times as the system is cooled towards T_g. The incoherent intermediate scattering function $F_s(q=6.82,t)$ in Fig. 2(b) exhibits a two-step relaxation at temperatures below the onset of caging. It is well established for supercooled liquids[77] that the short-time decay, the plateau, and the long-time decay can be attributed to vibrations, the β regime, and the α regime, respectively. The average relaxation time of the α process, τ_α, can be characterized by the $1/e$ decay time of $F_s(q,t)$. MCT predicts that the temperature dependence of τ_α is well described by a power law $\tau_\alpha \sim (T-T_{\mathrm{MCT}})^{-\gamma}$, from which the mode-coupling critical temperature T_{MCT} can be estimated. Accordingly, the power-law fit to our data yields $T_{\mathrm{MCT}}\approx 0.4$ as found in Ref. 72.

Next we show the average properties of mobile particles in the Dzugutov liquid so as to be able to compare their behavior with that of other glass-forming liquids. We first explore whether the mobile particles in the Dzugutov liquid form clusters. At any time interval Δt, we identify highly mobile particles by monitoring the displacements of all particles within this time window and, as in prior works,[9,10,16] we select 5% of the particles with the largest displacements. Following previous work,[16,19] we define a cluster as a group of highly mobile particles that are within the first neighbor shell of each other, where the first neighbor shell is defined by the distance of the first minimum of $g(r)$, cf. Fig. 1(b).

Figure 3 shows several typical clusters obtained at $T=0.42$. Obviously, there are a variety of clusters that have different shapes and sizes, so that a statistical analysis is necessary to determine the transient nature and T dependence of the clusters. We calculate $P(n(\Delta t))$, the probability of finding a cluster of size n at a time interval Δt, and from this, we compute the average cluster size. The weight-averaged mean cluster size $S(\Delta t)$ can be obtained using the relation[78]

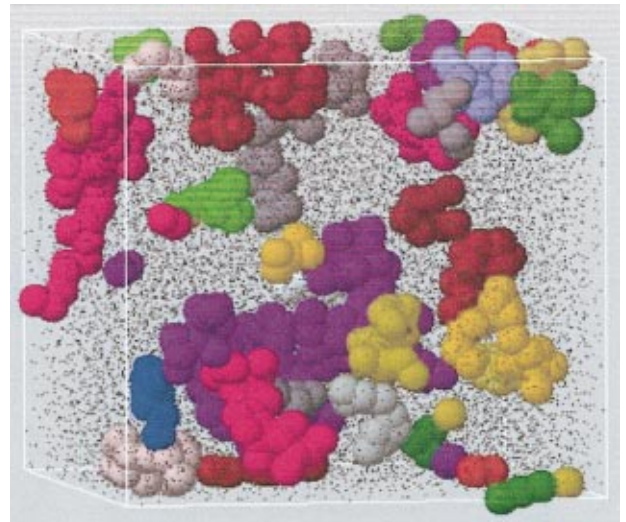$$S(\Delta t)=\frac{\sum n^2 P(n(\Delta t))}{\sum n P(n(\Delta t))}. \tag{2}$$

FIG. 3. (Color) Example of typical clusters formed by the 5% most mobile particles that are found at $T=0.42$ at the time $\Delta t=102.4$. Particles belonging to the same cluster are colored the same. Note that in the simulation all particles have the same size, but for the purpose of visualization all particles not in the subset studied are shown as dots.
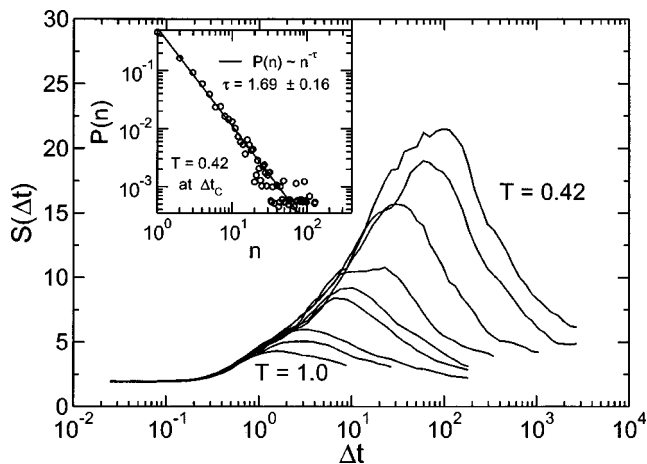
FIG. 4. The mean cluster size S as a function of time Δt for temperatures, from left to right, $T=1.0, 0.75, 0.65, 0.55, 0.52, 0.49, 0.46, 0.43,$ and 0.42. (Inset) Probability distribution, $P(n)$, at the time Δt_C for $T=0.42$. The solid line is a power law fit $P(n) \sim n^{-\tau}$. τ is found to be $\tau=1.69\pm0.16$.

In Fig. 4, we depict $S(\Delta t)$ for different T. It can be seen clearly that the mean cluster size increases rapidly upon cooling towards T_{MCT}. Moreover, $S(\Delta t)$ shows a peak at an intermediate time Δt_C that coincides with the time of the MSD crossover from the caging regime to the diffusive regime, cf. Fig. 2. We extract Δt_C for each T, and fit the data by a power law $\Delta t_C \propto (T-T_{MCT})^{-x}$ as was done in Ref. 19 for a supercooled polymer melt. It is evident from Fig. 5 that a power law, with an exponent $x=1.39\pm0.17$, yields a reasonable fit for the Dzugutov liquid. Within the estimated numerical error, this is consistent with $x=1.47\pm0.16$ observed in simulations of a polymer melt.[19] Thus, the transient nature of $S(\Delta t)$ is similar to that found in previous studies including experimental work on colloids.[28] In all cases studied, the peak of $S(\Delta t)$ lies in the late-β/early-α relaxation regime of
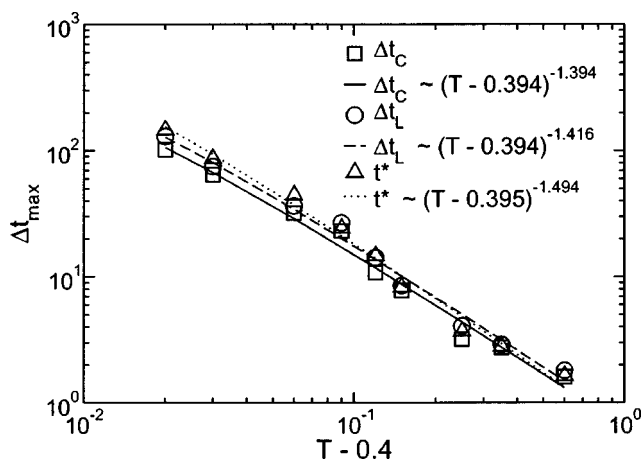

FIG. 5. Temperature dependence of the peak times Δt_C and Δt_L characterizing the times when the mean cluster size and the mean string size, respectively, are maximum. For completeness, the time t^* when the non-Gaussian parameter (not shown) of this system is maximum is also plotted. In the figure, the lines show results from nonlinear curve fitting of each data point to a power law $\sim (T-T_{MCT})^{-\gamma}$, where T_{MCT} and γ are used as free fit parameters. In all cases T_{MCT} is close to $T=0.4$.
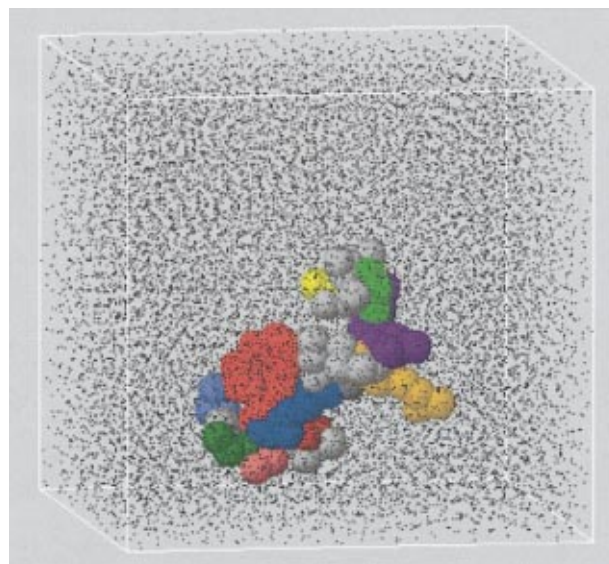

FIG. 6. (Color) Large cluster identified at $T=0.42$ at a time $\Delta t=102.4$. For the purpose of visualization all particles in the cluster are represented by a sphere of radius 1.0, while all other particles in the system are represented by a sphere of radius 0.1. Particles moving in the same string are given the same color. Those particles in the cluster that are not involved in string-like motion are colored gray.

the MCT and, hence, the dynamical process which manifests itself in the formation of the clusters precedes the long-time structural relaxation.

Another interesting similarity between different systems becomes obvious when inspecting the probability distribution of the cluster size. In accordance with previous works,[16,19,28] Fig. 4 shows that $P(n)$ at the characteristic time Δt_C is well described by a power law $P(n) \propto n^{-\tau}$ (multiplied by an exponential cutoff for $T>T_{MCT}$).[78] The exponent $\tau=1.69\pm0.16$ for the Dzugutov liquid at $T=0.42$ is similar to that found for a polymer melt ($\tau=1.62\pm0.12$) close to T_{MCT},[19] but it is different from the values obtained for a binary LJ mixture ($\tau=1.9$)[16] and a colloidal system ($\tau=2.2\pm0.2$).[28] Although the value of the exponent τ may be nonuniversal, it is noteworthy that, for all systems studied so far, the distribution $P(n)$ at the characteristic time Δt_C exhibits a power-law behavior when $T \to T_{MCT}$. We note that classical percolation theory[78] implies $\tau>2$. In contrast, $\tau<2$ was observed in all computational approaches. It has been argued[19] that this discrepancy may result from the finite system size and/or the intrinsically dynamic nature of the clusters in contrast to the static nature of the clusters in percolation theory. On the other hand, $\tau=1.4\pm0.15$ was also reported in experimental work on static clusters.[79] Further, considering the relatively large size of the present system we expect $P(n)$ to be only weakly affected by the system size in the studied T range.

A closer inspection reveals that the clusters, especially the larger ones, contain several strings, i.e., groups of particles that follow each other in quasi-one-dimensional paths.[10] This decomposition of the clusters is clearly seen in Fig. 6 where the different colors indicate distinct strings. To identify the strings we compare snapshots of the particle configurations at two different times, say at some reference time t
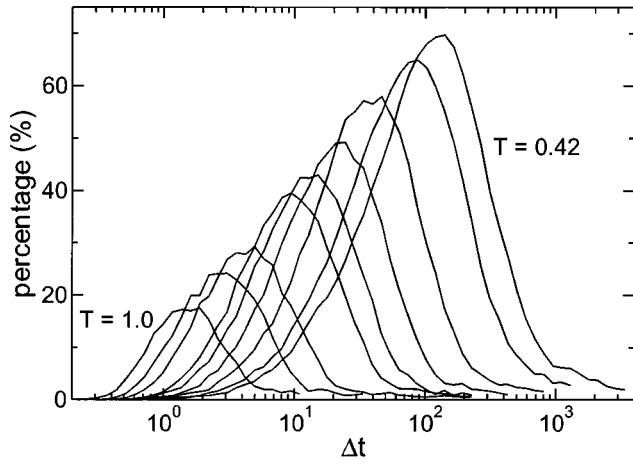
FIG. 7. The fraction $f(\Delta t)$, expressed in percentage, of mobile particles that move in nontrivial strings for temperatures $T = 1.0$, 0.75, 0.65, 0.55, 0.52, 0.49, 0.46, 0.43, and 0.42.

FIG. 8. The mean string size L as a function of time Δt for temperatures, from left to right, $T = 1.0$, 0.75, 0.65, 0.55, 0.52, 0.49, 0.46, 0.43, and 0.42. (Inset) Probability distribution, $P(l)$, at the time Δt_L for $T = 0.42$. The solid line represents an exponential fit, $P(l) \sim \exp(-l/l_o)$, where l_o is found to be $l_o = 2.38 \pm 0.24$.

$= t_0$ and at a later time $t = t_0 + \Delta t$, and search for mobile particles that have replaced neighboring mobile particles within a radius δ[10]. More precisely, we construct strings by connecting any two mobile particles i and j if $\min[|\mathbf{r_i}(t_0 + \Delta t) - \mathbf{r_j}(t_0)|, |\mathbf{r_i}(t_0) - \mathbf{r_j}(t_0 + \Delta t)|] < \delta$. Following Donati et al.[10] we used $\delta = 0.6$ for our analysis. Although the choice of δ is somewhat arbitrary, a different choice does not affect the qualitative features of our results, provided δ is chosen smaller than the particle radius σ. In fact, this has been confirmed in Ref. 20, where the mean string length was calculated for different δ.

As found also for a LJ mixture in Ref. 10, there are some mobile particles in the clusters that are not involved in string-like motion according to the criterion used. We thus wish to ascertain the relevance of string-like motion for relaxation in the highly mobile domains of the system. To address this issue, we compute the fraction $f(\Delta t)$ of mobile particles that are involved in nontrivial string-like motion, which means strings consisting of three or more particles. Figure 7 shows that the fraction grows significantly when T is decreased. For example, at Δt_C, roughly 70% of the mobile particles are involved in string-like motion for $T = 0.42$. Further, $f(\Delta t)$ has a maximum at a temperature-dependent time $\Delta t_f \approx \Delta t_C$, cf. Fig. 4. These results indicate that string-like motion is an important channel for the relaxation of mobile particles and becomes increasingly significant with decreasing T.

In analogy to the mean cluster size, the weight-averaged mean string length, L, can be calculated as a function of time and temperature

$$L(\Delta t) = \frac{\Sigma l^2 P(l(\Delta t))}{\Sigma l P(l(\Delta t))}, \tag{3}$$

where l is the number of particles in a string and $P(l(\Delta t))$ is the probability to find a string of length l in the time interval Δt. In Fig. 8, $L(\Delta t)$ is displayed for different T. The time and the temperature dependence of the mean string length are essentially similar to that of the mean cluster size. In particular, $L(\Delta t)$ peaks at a time Δt_L which is within the numerical error of Δt_C, and the maximum value of $L(\Delta t)$
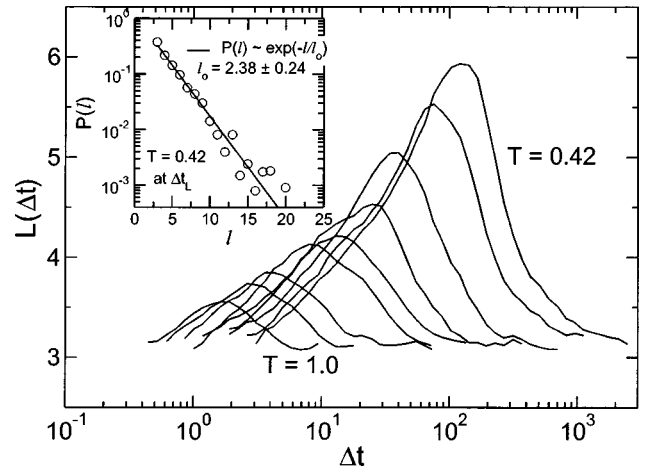
increases with decreasing T. Thus, long strings are mainly formed in the late-β/early-α relaxation regime where the mean length increases upon cooling. This time regime also corresponds to the time t^* when the non-Gaussian parameter $\alpha_2(t)$ is maximum (not shown). An important difference between strings and clusters exists for the respective size distributions. At the respective peak times for $T = 0.42$, $P(n)$ is well described by a power law (cf. Fig. 4) while $P(l)$ shows an exponential decay. Such behavior was also found in simulations for a binary LJ mixture[10] and a polymer melt,[20] where a detailed study on the transient nature and T dependence of string-like motion has been performed in association with polymer specific effects of bulk relaxation. As pointed out in Ref. 10, the observed exponential behavior is analogous to that reported for equilibrium polymerization[80–82] of linear polymer chains, in which the bonds between monomers break and recombine at random points along the backbone of the chain.

IV. MECHANISM OF STRING-LIKE MOTION

Thus far, we have explored the average properties of strings, and have shown that string-like motion is an important channel for relaxation in the domains of mobile particles in this model liquid. In this section we investigate further the details of string-like motion beyond what the length distribution and mean length reveal. What we intend to accomplish is to trace the string-like motion with an increasing amount of microscopic detail, in order to understand precisely how particles move in strings. In doing so, we study a number of issues relevant for cage rearrangement, cooperative motion, and dynamical heterogeneity.

As we have seen, strings are largest at times in the late-β/early-α relaxation regime of the MCT, indicating that the motion of mobile particles is highly cooperative on this time scale. However, the mechanism by which this cooperativity is realized is not apparent, i.e., the strings found at Δt_L may result from a series of local rearrangements at shorter times.
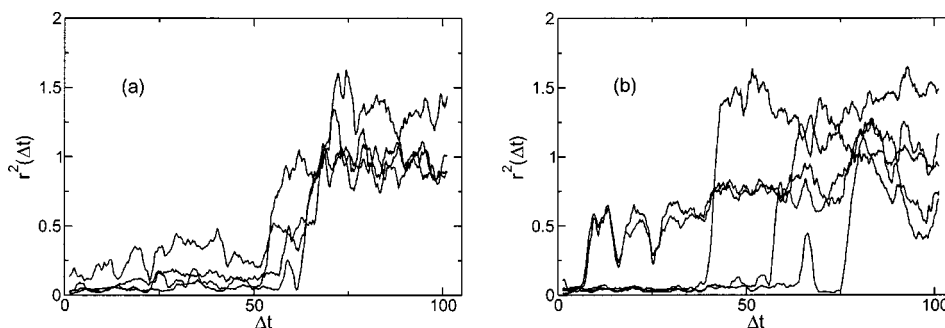
FIG. 9. Square displacement $r_i^2(\Delta t)$ of particles in strings that represent typical examples of (a) coherent motion and (b) noncoherent motion. Note that here, and in all other figures in this section depicting displacements of particles, the data have been smoothed using running averaging scheme in which several successive data points are replaced by their average to remove vibrational motion. Each data point is an average of 40 successive data points (equivalent to 200 MD steps) or a time range of $\Delta t = 2$.

For example, one can imagine that the strings are formed as a result of: (i) a "coherent" type of motion where all particles in a string move simultaneously in a single event, or in a time interval shorter than the dephasing time of the rattling motions within the local cages; (ii) a sequential type of motion where the particles in a string follow each other in a strictly ordered manner along the "backbone" of the string, i.e., the head of the string moves first and the tail last, but at relatively widespread time intervals; or (iii) a nonsequential, temporally random type of motion where single events in which the individual particles move into available empty space dominate on short time scales before some structured path emerges. Of course, the actual mechanism may also be a combination of all these processes where the prevailing mechanism depends on both the temperature and the length of the string. This is what we aim to determine in this section.

To investigate these processes, we first examine the individual motion of particles in strings, where we assess the squared displacement of each particle in the strings. Then, we investigate the relative motion of pairs of particles in strings that replace each other, where the relative motion is either with respect to their current positions or the original position of the replaced particle in the pair. In all cases we begin our analysis by inspecting several representative strings. Then, we calculate various ensemble averaged quantities to obtain information about the typical behavior. To do this, we first identify strings in the time interval Δt_L from some reference time t_0. Then, starting from the origin of this time interval we monitor the trajectories of the particles during the formation of the strings.

A. Analysis of typical examples

1. Single particle motion

First, we assess the individual motion of particles in strings during the formation of the strings by showing the square displacements of the constituting particles, $r_i^2(\Delta t)$, for two typical examples, see Fig. 9. For the string considered in Fig. 9(a), all particles move together within a short period of time by about one interparticle distance along a single path to replace the neighboring particle, suggesting a nearly coherent type of motion. In contrast, for the string studied in Fig. 9(b), two particles move forward as a pair,

whereas the jumps of the other particles occur individually at later times. In particular, the delay between the individual jumps is much larger than the dephasing time due to the cage-rattling motions for which an estimate, based on the onset of the plateau regime of the MSD, yields $\Delta t_{ph} \approx 5$, cf. Fig. 2. Thus, the motion of particles in this string is not coherent.

As can be seen in Fig. 10, the situation becomes even more complicated for large strings. In this figure, the square displacements $r_i^2(\Delta t)$ of the individual particles constituting one large string are organized in three panels to emphasize that subunits of the string, which we call "microstrings," can be identified within which the particles move nearly simultaneously. For example, the particles labeled 6, 7, 8, 9, and 10 jump together as a unit nearly at the same time, while the motions of the other subunits occur at different times. All these examples show that the string-like motion realized at some time Δt_L is a consequence of diverse processes at shorter times, some of which are coherent and some of which are not. To unveil these complicated processes we next inspect the motion of pairs of particles within strings in which one is replaced by the other ("replacing pairs").

2. Replacing pairs

According to their definition, strings consist of pairs of mobile particles in which one particle replaces the other in a time interval Δt. Valuable insights into the mechanism of string-like motion can be derived by inspecting the relative motions of these pairs. Suppose particles i and j constitute such a pair in a string k that has been identified in a time interval Δt_L, and let us further assume that j replaces i, i.e., the condition $dr_{ij}(\Delta t_L) < \delta \equiv 0.6$ is satisfied, where $dr_{ij}(\Delta t_L) \equiv |\mathbf{r}_j(t_0 + \Delta t_L) - \mathbf{r_i}(t_0)|$. Then, the calculation of $dr_{ij}(\Delta t < \Delta t_L)$ for all pairs in a string and identification of the times when each pair first satisfies the criterion $dr_{ij}(\Delta t) < \delta$ shows when the individual replacements in the string take place. Therefore, in this section we show $dr_{ij}(\Delta t)$ for all pairs in a typical string found at Δt_L, and then inspect the replacement mechanisms.

Figure 11 depicts the plot of $dr_{ij}(\Delta t)$ in the time window between t_0 and $t_0 + \Delta t_L$. A number of issues can be understood from the figure. Apparently, the replacements occur as sudden jumps, where for this string some of the jumps
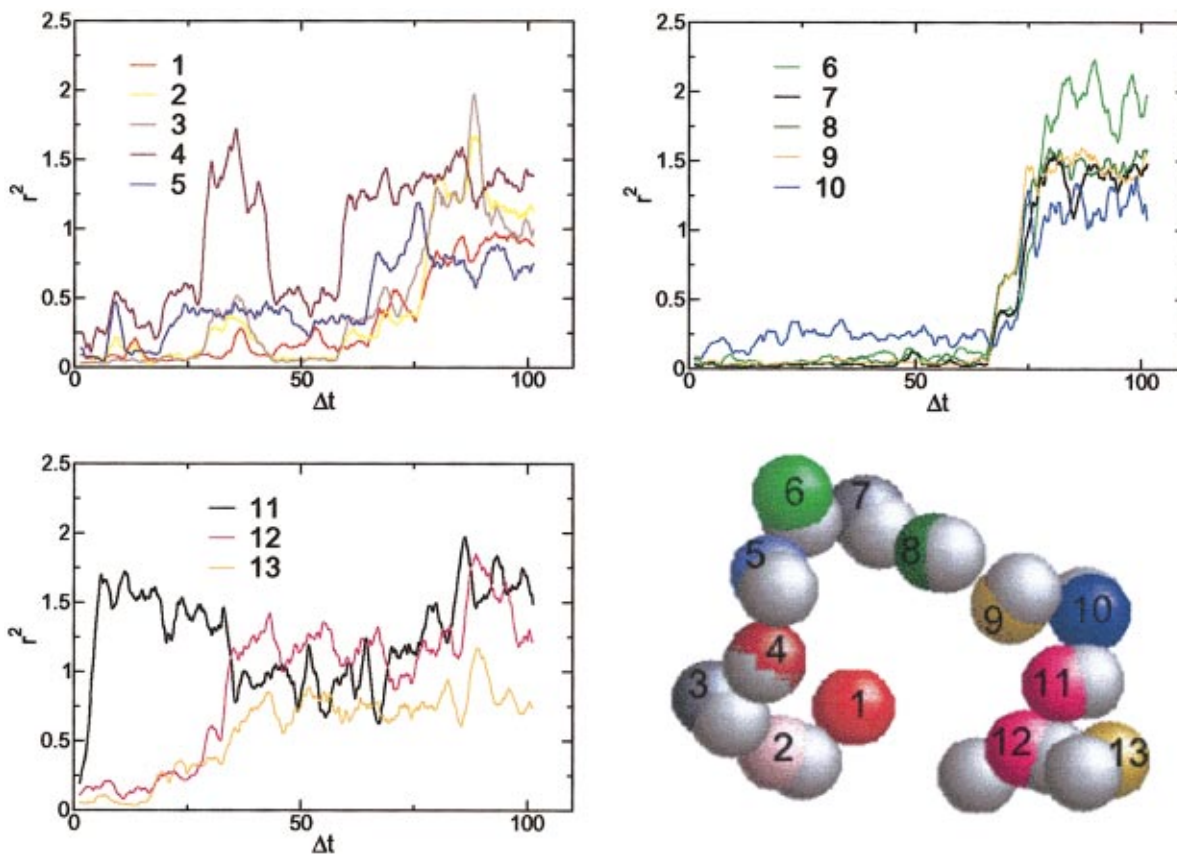
FIG. 10. (Color) The square displacement $r_i^2(\Delta t)$ of particles in a large string. Those particles that are moving together are grouped in the same panel. We refer to these subunits as microstrings. The position of particles in the string at the times t_0 and $t_0 + \Delta t_L$ are shown by spheres, where the numbered spheres represent positions at Δt_L and the remaining gray spheres represent the positions of the corresponding particles at the reference time t_0.

take place in groups (e.g., pairs 2, 3, and 4) at about the same time, while others (e.g., 5, 6, and 7) are well separated in time. Occasionally, we also observe unsuccessful replacement attempts (e.g., pair 7), where the replacing particle returns to its initial position prior to the jump, before the successful replacement eventually takes place at a later time t
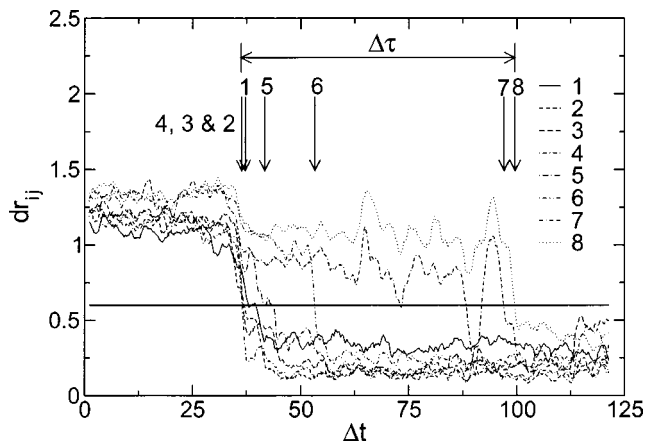

FIG. 11. A plot of $dr_{ij}(\Delta t) \equiv |\mathbf{r_j}(t_0 + \Delta t) - \mathbf{r_i}(t_0)|$, which characterizes the time when the condition $dr_{ij}(\Delta t_L) < \delta \equiv 0.6$ is first satisfied for any pair i, j in a particular string, i.e., the time when particle i is replaced by particle j. The pairs are labeled with a number describing their positions in the string from head to tail, where the pair at the head is labeled 1 and the pair at the tail is 8.

$<t_0 + \Delta t_L$. When this happens, we select the time of the final successful jump as the replacement time in the following analysis. By inspecting the duration $\Delta\tau$ (cf. Fig. 11) required for all pairs in a string to undergo successful replacement jumps, we can ascertain if the motion is coherent or not. If these jumps occur at once or within a short period of time, then we conclude that the motion is coherent, or simultaneous. Clearly, for the string analyzed, the motion is noncoherent since the replacements occur at widely separated times, and $\Delta\tau \approx 62$ is much longer than the dephasing time. Nevertheless, the string contains a subunit or microstring that moves simultaneously, as was recognized in the last subsection using a different approach.

When the motion within a string is noncoherent, we can further investigate whether or not the string-like motion involves sequential jumps of the constituting particles along the "backbone" of the string. This can be achieved by observing the time sequence of the replacement jumps in comparison to the pairs' order along the backbone of the string. However, due to partial coherent motion, as seen in pairs 2, 3, and 4 of Fig. 11, the identification of sequential motion becomes complicated, since for these pairs the sequence becomes indistinguishable or the order irrelevant because the pairs jump together almost at once. In any case, to gain some insight, we define sequential motion for strictly ordered jumps. That means only those strings that show replacement jumps in a strict order from head to tail are considered as
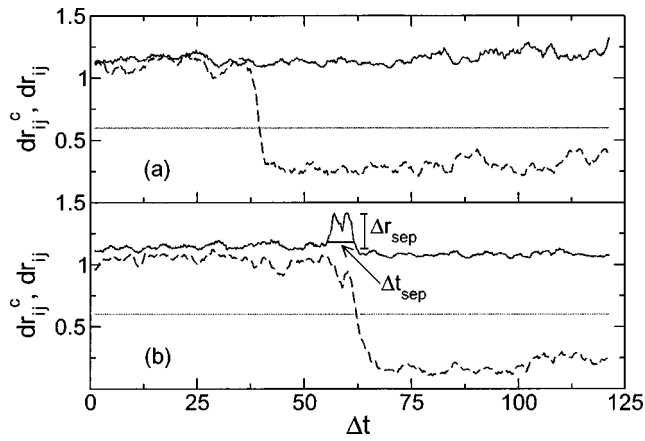
FIG. 12. The relative motion $dr_{ij}^c(\Delta t)$ (solid lines) of replacing pairs that are moving (a) coherently and (b) noncoherently. The separation time and the separation distance between the replacing pairs are indicated by Δt_{sep} and Δr_{sep}, respectively. To mark the time when the replacement jumps took place, we plot $dr_{ij}(\Delta t)$ (dashed line) for each pair. The horizontal lines mark the distance $dr_{ij}=0.6$.

FIG. 13. Probability distribution $P(\Delta\tau)$, where $\Delta\tau$ is the time between the first and the last replacement jumps in a string (cf. Fig. 11). The filled circles show $P(\Delta\tau)$ for all strings, while the shaded and unshaded bars represent $P(\Delta\tau)$ for strings of length $l<7$ and $l\geq7$, respectively. The x axis of the two bars have been shifted from each other by $\Delta\tau=1.0$ for clarity. In the inset we show the extent of coherent motion when we analyze different string lengths separately. For those strings in which particles that are not moving simultaneously, we calculate the probability of strings that exhibit sequential type of motion.

displaying sequential motion. Thus, the string analyzed in Fig. 11 has a sequence in which 4, 3, and 2 move before 1, and hence the motion in this string is not considered sequential. However, we observe other examples that exhibit sequential motion. In the next section we perform a statistical analysis to quantify this and the other mechanisms.

In the above considerations, we based our analysis at the level of strings to determine the rearrangement mechanisms. For example, by measuring the time span $\Delta\tau$ of the replacement jumps in the whole string, we were able to examine whether the motion is coherent or not. However, with this approach we cannot distinguish those cases where the majority of the particles move simultaneously from those where all jumps are well separated in time. Consider, for example, a string that consists of n particles. If one of the n particles jumps at a much later time while all the others jump simultaneously, $\Delta\tau$ will be large simply because of the one particle with a delayed jump time. Hence, the motion will be interpreted as noncoherent although most involved particles move simultaneously. To capture this behavior, we re-examine the relative motion of particles in replacing pairs, but this time with respect to their current positions, i.e., we calculate $dr_{ij}^c(\Delta t)\equiv|\mathbf{r_j}(t_0+\Delta t)-\mathbf{r_i}(t_0+\Delta t)|$ for any pair i and j in any given string for which j replaces i. Notice that in our previous analysis the current position $\mathbf{r_j}(t_0+\Delta t)$ of particle j is compared to the original position $\mathbf{r_i}(t_0)$ of particle i, but not to the current position. With this approach we will be able to determine the probability of coherent motion at a level of replacing pairs.

In Fig. 12 we show examples of $dr_{ij}^c(\Delta t)$ for representative pairs in two strings. This figure also includes the plots of $dr_{ij}(\Delta t)$ for the corresponding pairs, to mark the jump times described above. If the jump for a given pair occurs simultaneously, the plot of $dr_{ij}^c(\Delta t)$ remains flat, as shown in Fig. 12(a), since the particles do not separate significantly during their motion. On the other hand, if the replacing particle waits some time before it jumps into the position vacated by a replaced particle, i.e., if the replacement process is
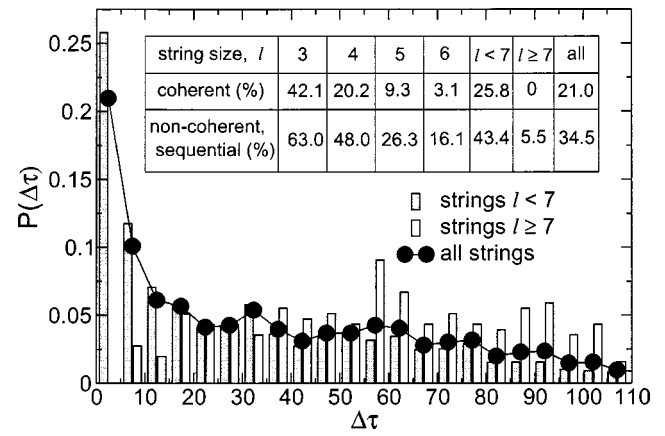
delayed, this plot shows, immediately preceding the jump time of the replacing particle, a bump in the plot of $dr_{ij}^c(\Delta t)$ [cf. Fig. 12(b) as an example]. Then, the height (Δr_{sep}) and the width (Δt_{sep}) of this bump [cf. Fig. 12(b)] characterize how far and how long the particles separate during the replacement process. From the time Δt_{sep} we can infer if a pair undergoes a coherent motion or not, while Δr_{sep} gives us additional information on the overall cage rearrangement. Clearly, the pair depicted by Fig. 12(a) exhibits a coherent jump, while the motion illustrated in Fig. 12(b) is noncoherent, since the jump of the replacing particle exhibits a significant delay.

B. Analysis of ensemble averaged quantities

Thus far, we have studied string-like motion by inspecting several representative examples. In this analysis, it has been demonstrated that the particle rearrangements involved in string-like motion result from a complex procedure involving different mechanisms. In order to determine the dominant mechanism, it is necessary to perform a statistical analysis. Therefore, we now calculate different probability distributions that quantify the average behavior.

We first show the probability distribution $P(\Delta\tau)$ of the time interval $\Delta\tau$ between the first and the last replacement jumps in a given string. In Fig. 13 we plot $P(\Delta\tau)$ obtained by averaging over all strings found in a time interval Δt_L, for $T=0.42$. This distribution quantifies the extent of coherent motion at a string level. As can be seen in the figure, $P(\Delta\tau)$ is a monotonically decreasing function of the time $\Delta\tau$.

To determine quantitatively the extent of coherent motion, we must assign a cutoff time interval below which the motion can be regarded as coherent. Ideally, we wish to define coherent motion as a process where the jumps occur at precisely the same time, but because this is an unlikely pro-

cess we must choose a reasonably small time that captures this event. In particular, this choice must be larger than the vibrational time scale, since we are interested only in rearrangements that contribute to string-like motion, and these are beyond the individual vibrations. Therefore, by inspecting the MSD or intermediate scattering function of the bulk (cf. Fig. 2), we define coherent or simultaneous motion as a process where all particles in a string undergo replacement jumps in a period $\Delta\tau < 5$. Based on this definition, we find that about 21% of the strings are moving simultaneously.

If we study small ($l<7$) and large ($l\geq7$) strings separately, we find different probability distributions. For the small strings, $P(\Delta\tau)$ is large for short time scales ($\Delta\tau<5$), while for the large strings no monotonic decay, but instead a broad distribution of $P(\Delta\tau)$, is observed. In particular, in terms of the criterion used to quantify the coherent motion, we find that none of the large strings ($l\geq7$) moves coherently when considering the motion of all particles in the string, whereas roughly 26% of the small strings ($l<7$) do. This probability grows to roughly 45% for the smallest string size, $l=3$ (see the inset of Fig. 13 for more details). These findings show that only small strings can move coherently as a unit whereas in large strings distinct subunits of the strings move at different times, resulting in an overall large time interval $\Delta\tau$ for the entire string, and hence implying a noncoherent type of motion at the level of strings. Nevertheless, we show later below that at the level of the individual subunits, or microstrings, the motion is coherent.

For those strings that do not move coherently, i.e., 79% of the strings, we quantify the relevance of sequential type of motion by counting those strings in which particles undergo strictly ordered jumps along the backbone of the string during a rearrangement process. We find that 35% of these strings exhibit sequential motion (cf. inset of Fig. 13), while 65% of the strings that are found to be noncoherent exhibit a nonsequential, temporally random motion in which one or more particles disrupt the ordered sequence of the replacement jumps. In fact, out of all strings, coherent as well as noncoherent, this amounts to nearly 51%. Therefore, nonsequential type of motion appears to be an important element of the string-like motion. If we further break down our analysis for different sizes, we find that sequential type of motion is more prevalent than nonsequential motion for smaller strings. For example, we find that about 63% of noncoherent strings of size $l=3$ undergo ordered jumps along the backbone of the strings, while only 9.2% of strings with size $l=7$ show strictly ordered jumps. Hence, as may be expected, strictly ordered replacements occur prevailingly for small noncoherent strings.

To gain further insight into the rearrangement mechanisms and to further establish the concept of microstrings, we will next discuss the statistical analysis done at the level of replacing pairs in strings. We first calculate the probability distribution $P(\Delta t_{sep})$ that characterizes the separation times Δt_{sep} between replacing particles. Figure 14(a) displays the probability distribution obtained by averaging over all replacing pairs in strings found at a time interval Δt_L for $T=0.42$. Similar to what we find from $P(\Delta\tau)$, $P(\Delta t_{sep})$ decays monotonically. If we integrate the probability distribu-
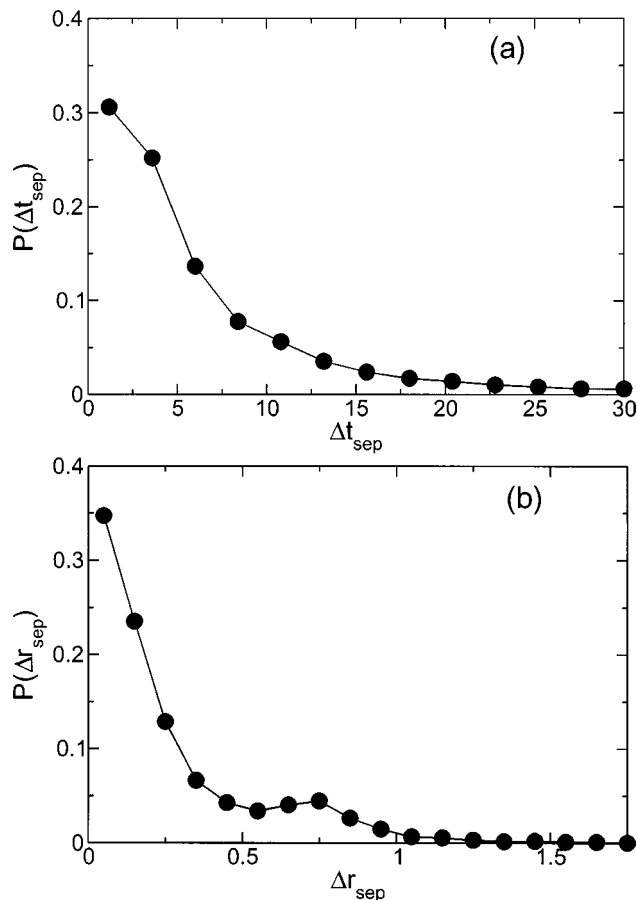

FIG. 14. Probability distributions of (a) the separation time Δt_{sep} and (b) the separation distance Δr_{sep} of replacing pairs during the replacement process.

tion up to a cutoff time $\Delta t_{sep} \approx 5$ for estimating the probability of coherent jumps in pairs, we find a value of 0.56. Therefore, about 56% of the replacing pairs move simultaneously in the replacement process. This number is significantly larger than that obtained by analyzing $P(\Delta\tau)$ (21%). The difference shows the presence of a substantial number of strings that have been counted as noncoherent, while the majority of the particles in these strings actually move simultaneously in microstrings. Therefore, the two probability distributions complement each other and, only in combination, give us complete information on the extent of coherent motion in strings.

Additional information about the rearrangement of particles in strings can be extracted by examining Fig. 14(b), which shows the probability distribution $P(\Delta r_{sep})$ of an excess separation distance Δr_{sep} between replacing pairs in a string during the replacement process. Questions such as, "By how much do particles separate from each other during the replacement process as compared to the size of the cage radius r_c?" can be studied. Clearly, high probability is attained for small separations, with the tail of the probability extending to $\Delta r_{sep} \approx 1$, i.e., one interparticle distance. In fact, most pairs have $\Delta r_{sep} < r_c$, where r_c can be estimated using three-time correlation functions.[83] As shown in the Appendix, this analysis yields $r_c \approx 0.45$ for the Dzugutov liquid at $T=0.42$, i.e., the cage radius is slightly smaller than the half interparticle distance, which is consistent with previous find-

ings for supercooled liquids.[41,83,84] Based on this estimate, an integration of $P(\Delta r_{sep})$ in the range $\Delta r_{sep} \lesssim r_c$ yields 0.81, suggesting that only 19% of the pairs separate by a distance larger than the cage radius during the replacement process. Since coherent motion leads to small pair separations, e.g., $\Delta r_{sep} \lesssim r_c$, the high probability in this region is again consistent with the previous finding that large strings typically consist of several microstrings in which the particles move simultaneously.

V. DISCUSSION AND CONCLUSION

We studied the microscopic dynamics in a glass-forming one-component supercooled liquid modeled by the Dzugutov potential. We found that a dominant mode of motion by highly mobile particles is string-like motion. To gain insight into the mechanism that leads to the emergence of strings we conducted a detailed investigation of the nature of string-like motion. For this purpose, we identified strings in a time interval Δt_L where their mean value shows a maximum, and traced the trajectories of the particles in the strings during this period of time. We monitored both the single particle motion and the relative motion of pairs in which one particle replaces the other. Inspecting the data for several representative examples we found that the string-like motion results from a complex interplay of diverse processes. Because of this diversity, we performed statistical analyses to determine the dominant mechanism of string-like motion.

We found that if one defines a string as coherent if and only if *all* particles within that string move simultaneously in a short period of time, then only 21% of the strings fall into this category, and they are typically small strings. For example, about half of the strings of length $l = 3$ show coherent motion. Noncoherent strings are found to exhibit particle motion that is both sequential, i.e., motion in which particles move in a strict order of head to tail along the backbone of the strings, but at widespread time intervals, and nonsequential or random motion. The extent of sequential motion in the noncoherent strings was found to be about 35%, from which temporally random, nonsequential motion was estimated to be about 65%. Thus, for most noncoherent strings, we find that individual particles or microstrings move in a nonsequential manner. In particular, sequential motion is usually not observed for long strings.

For a substantial number of noncoherent strings, simultaneous (coherent) motion is observed within small subunits of the strings, referred to as microstrings. Hence, there is coherent motion on shorter length scales. Quantifying the degree of coherence at the level of replacing pairs reveals that 56% of the particles in replacing pairs move simultaneously. In addition, only 19% of all replacing pairs separate by a distance larger than the cage radius during the replacement process. Thus at the level of replacing pairs the motion is for the most part coherent, whereas it is noncoherent at the level of strings. These observations show that intermediate or large strings are formed as a result of subsequent motion of smaller subunits, either single particles or microstrings, within which the particles move coherently. Individual microstrings are not coherent with each other. Thus, the replacement of a pair of particles becomes noncoherent in the

event when the two particles belong to two different subunits of the string, i.e., different microstrings. The present findings for the mechanism of string-like motion are consistent with the outcome of a study on the particle rearrangements resulting from the transitions between successively visited inherent structures of a binary LJ liquid.[60] There, it was observed that long strings identified after sequences of transitions do not result from a coherent motion of all particles during a single transition, but instead the particles replace each other at different times either in single-particle type motion or in small microstrings. Moreover, back-and-forth jumps of microstrings were observed.

Altogether, the following picture appears to emerge: On very short time scales, small groups of particles (microstrings) move together and, hence, the length scale of cooperative motion is small. At longer times, the interplay of these individual motions leads to the formation of larger and larger strings, which in turn aggregate into clusters. Within these dynamical objects, particles assist each other to escape from their respective cages and the length scale of cooperative motion becomes maximum at times in the late-β/early-α relaxation regime. At even later times, the cooperativity diminishes due to the independent diffusion of the particles. Along these lines, it may be suggested that—in analogy to the formation of the strings due to the concerted motion of smaller subunits—the growth of the clusters may be a consequence of the interplay of various strings. In other words, cooperativity on various time scales and length scales may be the basis of spatially heterogenous dynamics.

One may ask why the small length scale associated with the cooperativity of particle motion observed at short time scales increases and becomes organized into larger, quasi-one-dimensional objects in the late-β/early-α relaxation regime. Very recently Garrahan and Chandler[42] and Berthier and Garrahan[44,45] proposed that dynamics in a supercooled liquid can be understood via two simple ingredients, namely, the existence of spatially heterogeneous dynamics and the facilitation of dynamics in the vicinity of regions exhibiting high particle mobility. The mechanism for the formation of large strings resembles the concept of dynamic facilitation. In particular, one may speculate that the local excitations envisaged by Garrahan and Chandler are associated with the coherent motion of particles within microstrings, thereby facilitating the creation of neighboring excitations that extend throughout the string.

Another possible reason for string-like motion lies in the local static structure of a supercooled liquid. In a numerical study of a 2D monodisperse system of particles, Reichardt and Reichardt[85] found fluctuating topological defects that form a string-like structure. Although this observation has to be further investigated for a 3D system such as ours, weak one-dimensional fissures may possibly develop in the liquid, providing a path for string-like motion. Dzugutov *et al.*[73] established a relation between dynamical heterogeneity and structural heterogeneity for the studied model liquid. In particular, it was demonstrated that clusters of icosahedrally coordinated particles exist in the Dzugutov liquid where, on average, the particles inside and outside of an icosahedral environment show reduced and enhanced mobilities, respec-
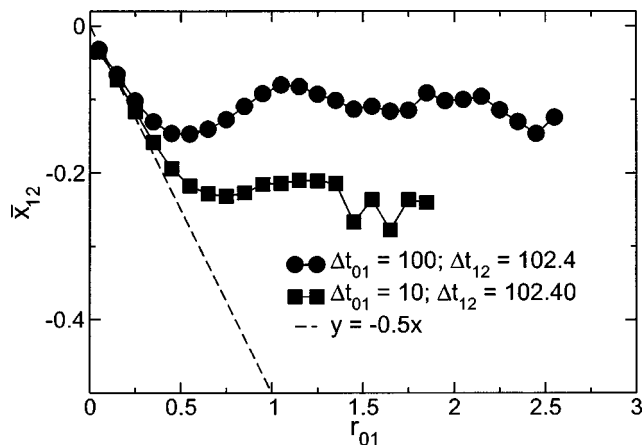
FIG. 15. Three-time correlation function $\bar{x}_{12}(r_{01})$ characterizing the motion of individual particles in two successive time intervals.

tively. Hence, one may speculate that string-like motion, at least in the Dzugutov liquid, is most pronounced in noni-cosahedral environments, e.g., in channels between clusters of icosahedrally coordinated particles. Indeed, preliminary results[86] suggest that string-like motion occurs primarily along the edges of such clusters. Further work along these lines is in progress.

ACKNOWLEDGMENTS

APPENDIX: ESTIMATE OF THE CAGE RADIUS r_c

Following Refs. 41, 83, and 84, we calculate three-time correlation function characterizing the motion of individual particles in two time intervals in order to estimate the cage size. Specifically, we measure the displacements $\mathbf{r_{01}}$ and $\mathbf{r_{12}}$ of the particles during successive time intervals Δt_{01} and Δt_{12}, and then calculate the projection of $\mathbf{r_{12}}$ on the direction of $\mathbf{r_{01}}$, i.e.,

$$x_{12} = \frac{\mathbf{r_{01}}}{r_{01}} \cdot \mathbf{r_{12}}, \tag{A1}$$

where $r_{01} \equiv |\mathbf{r_{01}}|$. Based on these data, we compute the conditional probability function $P(x_{12}|r_{01})$, which measures the probability to find a specific value x_{12} provided the particle has moved a distance r_{01} in the first time interval Δt_{01}. Information about the direction of subsequent steps of the motion can be extracted from the first moment of this distribution $\bar{x}_{12}(r_{01})$.[41,83,84] Specifically, $x_{12}(r_{01}) \equiv 0$ will result if the directions of the motions during Δt_{01} and Δt_{12} are uncorrelated. In contrast, if the subsequent motion for a given r_{01} is backward (forward) correlated, a negative (positive) value of $\bar{x}_{12}(r_{01})$ will be found. In particular, it has been

shown that $\bar{x}_{12}(r_{01}) = -\frac{1}{2}r_{01}$ results from stochastic dynamics in a harmonic potential.[87] Choosing the intervals Δt_{01} and Δt_{12} in the caging regime, these effects can be used to estimate the cage size for supercooled liquids.[41,83,84] Figure 15 shows $\bar{x}_{12}(r_{01})$ for $\Delta t_{01} = 10$, 100, and $\Delta t_{12} = 102.4$ at $T = 0.42$. Obviously, $\bar{x}_{12}$ is negative for all values of r_{01}. Thus, as a signature of the cage effect, on average a particle moves opposite to the direction it has moved before. For $r_{01} < r_c \approx 0.45$, the curves nicely follow $\bar{x}_{12}(r_{01}) = -\frac{1}{2}r_{01}$ indicating that the particle is dragged back by a constant fraction of its previous displacement. On the other hand, the back dragging effect decreases for $r_{01} > r_c$. Therefore the cage radius can be estimated to be $r_c \approx 0.45$.

[1] J. Jäckle, Rep. Prog. Phys. **49**, 171 (1986).
[2] W. Götze, in Proceedings of the Les Houches Summer School of Theoretical Physics, Les Houches 1989, Session LI, edited by J. P. Hansen, D. Levesque, and J. Zinn-Justin (North-Holland, Amsterdam, 1991), pp. 287–503.
[3] P. Lunkenheimer, U. Schneider, R. Brand, and A. Loidl, Contemp. Phys. **41**, 15 (2000).
[4] R. Böhmer, K. L. Ngai, C. A. Angell, and D. J. Plazek, J. Chem. Phys. **99**, 4201 (1993).
[5] C. A. Angell, Science **267**, 1924 (1995).
[6] M. D. Ediger, C. A. Angell, and S. R. Nagel, J. Phys. Chem. **100**, 13200 (1996).
[7] F. H. Stillinger and J. A. Hodgdon, Phys. Rev. E **50**, 2064 (1994).
[8] I. Chang and H. Sillescu, Phys. Rev. E **53**, 2992 (1996).
[9] W. Kob, C. Donati, S. J. Plimpton, P. H. Poole, and S. C. Glotzer, Phys. Rev. Lett. **79**, 2827 (1997).
[10] C. Donati, J. F. Douglas, W. Kob, S. J. Plimpton, P. H. Poole, and S. C. Glotzer, Phys. Rev. Lett. **80**, 2338 (1998).
[11] R. Yamamoto and A. Onuki, Phys. Rev. E **58**, 3515 (1998).
[12] D. N. Perera and P. Harrowell, J. Chem. Phys. **111**, 5441 (1999).
[13] J. Qian, R. Hentschke, and A. Heuer, J. Chem. Phys. **111**, 10177 (1999).
[14] S. C. Glotzer and C. Donati, J. Phys.: Condens. Matter **11**, A285 (1999).
[15] P. H. Poole, C. Donati, and S. C. Glotzer, Physica A **261**, 51 (1998).
[16] C. Donati, S. C. Glotzer, P. H. Poole, W. Kob, and S. J. Plimpton, Phys. Rev. E **60**, 3107 (1999).
[17] C. Bennemann, C. Donati, J. Baschnagel, and S. C. Glotzer, Nature (London) **399**, 246 (1999).
[18] B. Doliwa and A. Heuer, Phys. Rev. E **61**, 6898 (2000).
[19] Y. Gebremichael, T. B. Schrøder, F. W. Starr, and S. C. Glotzer, Phys. Rev. E **64**, 051503 (2001).
[20] M. Aichele, Y. Gebremichael, F. W. Starr, J. Baschnagel, and S. C. Glotzer, J. Chem. Phys. **119**, 5270 (2003).
[21] N. Giovambattista, S. V. Buldyrev, F. W. Starr, and H. E. Stanley, Phys. Rev. Lett. **89**, 125501 (2003).
[22] K. Schmidt-Rohr and H. W. Spiess, Phys. Rev. Lett. **66**, 3020 (1991).
[23] M. T. Cicerone and M. Ediger, J. Chem. Phys. **103**, 5684 (1995).
[24] B. Schiener, R. Böhmer, A. Loidl, and R. V. Chamberlin, Science **274**, 752 (1996).
[25] M. Yang and R. Richert, J. Chem. Phys. **115**, 2676 (2001).
[26] U. Tracht, M. Wilhelm, A. Heuer, H. Feng, K. Schmidt-Rohr, and H. W. Spiess, Phys. Rev. Lett. **81**, 2727 (1998).
[27] A. Marcus, J. Schofield, and S. Rice, Phys. Rev. E **60**, 5725 (1999).
[28] E. Weeks, J. C. Crocker, A. C. Levitt, A. Schofield, and D. A. Weitz, Science **287**, 627 (2000).
[29] W. K. Kegel and A. van Blaaderen, Science **287**, 290 (2000).
[30] M. Russina and F. Mezei, Phys. Rev. Lett. **84**, 3630 (2000).
[31] H. Sillescu, J. Non-Cryst. Solids **243**, 81 (1999).
[32] M. D. Ediger, Annu. Rev. Phys. Chem. **51**, 99 (2000).
[33] R. Richert, J. Phys.: Condens. Matter **14**, R703 (2002).
[34] U. Tracht, M. Wilhelm, A. Heuer, K. Feng, and H. Schmidt-Rohr, Phys. Rev. Lett. **81**, 2727 (1998).
[35] S. A. Reinsberg, X. H. Qiu, M. Wilhelm, H. W. Spiess, and M. D. Ediger, J. Chem. Phys. **114**, 7299 (2001).
[36] S. C. Glotzer, J. Non-Cryst. Solids **274**, 342 (2000).
[37] G. Adam and J. H. Gibbs, J. Chem. Phys. **43**, 139 (1965).
[38] H. Yin and B. Chakraborty, Phys. Rev. Lett. **86**, 2058 (2001).
[39] M. Russina and F. Mezei, Phys. Rev. B **276–278**, 437 (2000).

[40] B. Cui, B. Lin, and S. A. Rice, J. Chem. Phys. **114**, 9142 (2001).

[41] E. Weeks and D. A. Weitz, Phys. Rev. Lett. **89**, 095704 (2002).

[42] J. P. Garrahan and D. Chandler, Phys. Rev. Lett. **89**, 035704 (2002).

[43] J. P. Garrahan and D. Chandler, Proc. Natl. Acad. Sci. U.S.A. **100**, 9710 (2003).

[44] L. Berthier and J. P. Garrahan, cond-mat/0306469 (4 July 2003), Vol. 2.

[45] L. Berthier and J. P. Garrahan, J. Chem. Phys. **119**, 4367 (2003).

[46] G. H. Fredrickson and H. C. Andersen, Phys. Rev. Lett. **53**, 1244 (1984).

[47] G. H. Fredrickson and H. C. Andersen, J. Chem. Phys. **83**, 5822 (1985).

[48] Y. Gebremichael, M. Vogel, and S. C. Glotzer, Mol. Simul. (to be published).

[49] M. Goldstein, J. Chem. Phys. **51**, 3728 (1969).

[50] F. H. Stillinger, Science **267**, 1935 (1995).

[51] C. A. Angell, Science **267**, 1924 (1995).

[52] P. G. Debenedetti and F. H. Stillinger, Nature (London) **410**, 259 (2001).

[53] D. J. Wales *et al.*, Adv. Chem. Phys. **115**, 1 (2000).

[54] T. F. Middleton and D. J. Wales, Phys. Rev. B **64**, 024205 (2001).

[55] S. Büchner and A. Heuer, Phys. Rev. Lett. **84**, 2168 (2000).

[56] S. Büchner and A. Heuer, Phys. Rev. E **60**, 6507 (1999).

[57] B. Doliwa and A. Heuer, Phys. Rev. E **67**, 030501 (2003).

[58] T. B. Schrøder, S. Sastry, J. C. Dyre, and S. C. Glotzer, J. Chem. Phys. **112**, 9834 (2000).

[59] R. A. Denny, D. R. Reichman, and J.-P. Bouchard, Phys. Rev. Lett. **90**, 025503 (2003).

[60] M. Vogel, B. Doliwa, A. Heuer, and S. C. Glotzer, J. Chem. Phys. (to be published).

[61] R. J. Speedy, Mol. Phys. **95**, 169 (1998).

[62] A. Scala, F. W. Starr, E. L. Nave, F. Sciortino, and H. E. Stanley, Nature (London) **406**, 166 (2000).

[63] S. Sastry, Nature (London) **409**, 164 (2001).

[64] S. Mossa *et al.*, Phys. Rev. E **65**, 041205 (2002).

[65] M. Dzugutov, Phys. Rev. A **46**, R2984 (1992).

[66] M. Dzugutov, K. E. Larsson, and Ebbsjö, Phys. Rev. A **38**, 3609 (1988).

[67] A. Harrison, *Pseudopotential in the Theory of Metals* (Benjamin, New York, 1966).

[68] J. Roth and A. R. Denton, Phys. Rev. E **61**, 6845 (2000).

[69] S. Sachdev and D. Nelson, Phys. Rev. B **32**, 1480 (1985).

[70] J. Hafner, *From Hamiltonian to Phase Diagram* (Springer, Berlin, 1987).

[71] D. Nelson, Phys. Rev. B **28**, 5515 (1983).

[72] F. Zetterling, M. Dzugutov, and S. Simdyankin, J. Non-Cryst. Solids **39**, 293 (2001).

[73] M. Dzugutov, S. I. Simdyankin, and F. H. M. Zetterling, Phys. Rev. Lett. **89**, 195701 (2002).

[74] M. Dzugutov, Phys. Rev. Lett. **70**, 2924 (1993).

[75] S. Simdyankin, M. Dzugutov, S. N. Taraskin, and S. R. Elliott, Phys. Rev. B **63**, 184301 (2001).

[76] J. P. K. Doye, Faraday Discuss. **118**, 159 (2001).

[77] W. Kob and H. C. Andersen, Phys. Rev. E **51**, 4626 (1995).

[78] D. Stauffer, *Introduction to Percolation Theory* (Taylor and Francis, London, 1985).

[79] G. K. Schulthess, G. B. Benedek, and R. W. De Blois, Macromolecules **13**, 939 (1980).

[80] R. Bellissent, L. Descotes, and P. Pfeuty, J. Phys.: Condens. Matter **6**, A211 (1994).

[81] Y. Rouault and A. Milchev, Phys. Rev. E **51**, 5905 (1995).

[82] S. C. Greer, Adv. Chem. Phys. **94**, 261 (1996).

[83] B. Doliwa and A. Heuer, Phys. Rev. Lett. **80**, 4915 (1998).

[84] B. Doliwa and A. Heuer, J. Phys.: Condens. Matter **11**, A277 (1999).

[85] C. Reichhardt and C. J. Reichhardt, Phys. Rev. Lett. **90**, 095504 (2003).

[86] M. Bergroth, A. S. Keyes, M. Vogel, Y. Gebremichael, and S. C. Glotzer (unpublished results).

[87] A. Heuer, M. Kunow, M. Vogel, and R. D. Banhatti, Phys. Rev. B **66**, 224201 (2002).